REPORT DOCUMENTATION PAGE

Form Approved
OMB No. 0704-0188

1. REPORT DATE *(DD-MM-YYYY)*	2. REPORT TYPE	3. DATES COVERED *(From - To)*
30-DEC-2014	Final	Feb 2013 to Dec 2014

4. TITLE AND SUBTITLE
Implementation of a Particle Image Velocimetry System for Wind Tunnel Flowfield Measurements

5a. CONTRACT NUMBER

5b. GRANT NUMBER

5c. PROGRAM ELEMENT NUMBER
OH

6. AUTHOR(S)
Kevin Kimmel, Paisan Atsavapranee, Anish Sydney, Joseph Ramsey, Matthew Marquardt, Emily Harrison

5d. PROJECT NUMBER

5e. TASK NUMBER

5f. WORK UNIT NUMBER
300000076527

7. PERFORMING ORGANIZATION NAME(S) AND ADDRESS(ES) AND ADDRESS(ES)

Naval Surface Warfare Center
Carderock Division
9500 Macarthur Boulevard
West Bethesda, MD 20817-5700

8. PERFORMING ORGANIZATION REPORT NUMBER

NSWCCD-80-TR-2014/045

9. SPONSORING / MONITORING AGENCY NAME(S) AND ADDRESS(ES)
NSWC-CD NISE Program
(Section 219)

10. SPONSOR/MONITOR'S ACRONYM(S)

11. SPONSOR/MONITOR'S REPORT NUMBER(S)

12. DISTRIBUTION / AVAILABILITY STATEMENT
Approved for public release; distribution is unlimited.

13. SUPPLEMENTARY NOTES

14. ABSTRACT

A test program was planned and conducted to implement Particle Image Velocimetry (PIV) as a flow measurement technique in the 8′ x 10′ Subsonic Wind Tunnel at Naval Surface Warfare Center, Carderock Division using Naval Innovative Science and Engineering funding. The test was designed to examine the flowfield and airwake of a generic ship geometry that was tested previously, enabling the comparison of PIV results to velocity probe measurements from the prior investigation. In addition to PIV, Stereo Particle Image Velocimetry (SPIV), a more advanced variant, was performed. The ship model was oriented at a 0-deg heading with respect to wind direction (heading into the wind), and measurements were taken at flow velocities of 30, 60, and 90 knots. Data were collected along longitudinal planes aligned with the model heading, as well as from one lateral plane that cut across the flight deck. Test results are discussed and summarized. PIV and SPIV were successfully demonstrated in the wind tunnel, and are now available as powerful flowfield measurement tools for future test programs.

15. SUBJECT TERMS
Particle Image Velocimetry, PIV, SPIV, wind tunnel, airwake, SFS2, flow seeding, flow survey

16. SECURITY CLASSIFICATION OF:			17. LIMITATION OF ABSTRACT	18. NUMBER OF PAGES	19a. NAME OF RESPONSIBLE PERSON
a. REPORT	b. ABSTRACT	c. THIS PAGE			Kevin R. Kimmel
UNCLASSIFIED	UNCLASSIFIED	UNCLASSIFIED		40	19b. TELEPHONE NUMBER *(include area code)* 301-227-1584

20150319174

DEPARTMENT OF THE NAVY
NAVAL SURFACE WARFARE CENTER
CARDEROCK DIVISION

CARDEROCK DIVISION HEADQUARTERS
DAVID TAYLOR MODEL BASIN
9500 MACARTHUR BOULEVARD
WEST BETHESDA, MD 20817-5700

IN REPLY REFER TO:

5605
Ser 850/015
13 March 2015

From: Commander, Naval Surface Warfare Center, Carderock Division
To: Defense Technical Information Center

Subj: FORWARDING OF REPORT

Encl: (1) NSWCCD-80-TR-2014/045, "Implementation of a Particle Image Velocimetry System for Wind Tunnel Flowfield Measurements" by Kevin Kimmel, Paisan Atsavapranee, Anish Sydney, Joseph Ramsey, Matthew Marquardt and Emily Harrison, December 2014

1. Enclosure (1) is forwarded for your information and retention.

2. For questions, please contact Kevin Kimmel at 301-227-1584, or email, kevin.kimmel@navy.mil.

STEPHEN EBNER
By direction

Naval Surface Warfare Center
Carderock Division
West Bethesda, MD 20817-5700

NSWCCD-80-TR-2014/045 December 2014
Naval Architecture and Engineering Department Report

Implementation of a Particle Image Velocimetry System for Wind Tunnel Flowfield Measurements

By

Kevin Kimmel
Paisan Atsavapranee
Anish Sydney
Joseph Ramsey
Matthew Marquardt
Emily Harrison

CONTENTS

FIGURES

TABLES

LIST OF ABBREVIATIONS

C	*Celsius*
CCD	*Charged Coupled Device*
CL	*Centerline*
deg	*Degrees*
F	*Fahrenheit*
FRP	*Fast-response probe*
ft	*Feet*
ft/s	*Feet per second*
H	*Height of the hangar above the flight deck*
Hz	*Hertz*
in.	*Inch*
m	*meters*
mJ	*Millijoules*
mm	*Millimeters*
m/s	*Meters per second*
NISE	*Naval Innovative Science and Engineering*
NSWCCD	*Naval Surface Warfare Center, Carderock Division*
PIV	*Particle Image Velocimetry*
psi	*Pounds per square-inch*
psia	*Pounds per square-inch absolute*
ROI	*Region of Interrogation*
SFS1	*Simple Frigate Shape 1*
SFS2	*Simple Frigate Shape 2*
SPIV	*Stereo Particle Image Velocimetry*
SWT	*Subsonic Wind Tunnel*
TTCP	*The Technical Cooperation Panel*
u	*Wind velocity component in the x direction*
v	*Wind velocity component in the y direction*
V	*Volts*
V_{inf}	*Freestream wind velocity*
V_{xz}	*Velocity calculated from x and z velocity components (no y component)*
w	*Wind velocity component in the z direction*
ω_{xz}	*Vorticity in the x-z plane*
ω'_{xz}	*Vorticity calculated from the fluctuating component of velocity in the x-z plane*
Δt	*Offset in time between firing of lasers*
μ s	*Microseconds*
2-D	*Two dimensional*

ABSTRACT

A test program was planned and conducted to implement Particle Image Velocimetry (PIV) as a flow measurement technique in the 8' x 10' Subsonic Wind Tunnel at Naval Surface Warfare Center, Carderock Division using Naval Innovative Science and Engineering funding. The test was designed to examine the flowfield and airwake of a generic ship geometry that was tested previously, enabling the comparison of PIV results to velocity probe measurements from the prior investigation. In addition to PIV, Stereo Particle Image Velocimetry (SPIV), a more advanced variant, was performed. The ship model was oriented at a 0-deg heading with respect to wind direction (heading into the wind), and measurements were taken at flow velocities of 30, 60, and 90 knots. Data were collected along longitudinal planes aligned with the model heading, as well as from one lateral plane that cut across the flight deck. Test results are discussed and summarized. PIV and SPIV were successfully demonstrated in the wind tunnel, and are now available as powerful flowfield measurement tools for future test programs.

ADMINISTRATIVE INFORMATION

The work described in this report was performed by the Marine and Aviation Division (Code 88) with the assistance of the Submarine Maneuvering and Control Division (Code 86) and the Surface Ship Hydromechanics Division (Code 85), all of which are part of the Naval Architecture and Engineering Department at the Naval Surface Warfare Center, Carderock Division (NSWCCD). This work was performed under funding through the Naval Innovative Science and Engineering (NISE) program and administered by the NSWCCD Director of Research. Testing was done over the period June 2014 through July 2014.

ACKNOWLEDGMENTS

The authors would like to acknowledge the efforts of Josh Rollins for his contributions to the design, setup, and conduct of the wind tunnel test program. The authors would also like to thank Monica Walker as well as the Naval Architecture and Engineering Department technicians for their contributions during the test.

INTRODUCTION

Ship topside design directly determines the surrounding aerodynamic flowfield in which aircraft operate during launch and recovery operations. Detailed experimental measurements are needed to evaluate ship topside aerodynamics and to validate computational tools. Flowfield measurement capability in the NSWCCD 8' x 10' Subsonic Wind Tunnel (SWT) has been limited to pressure probes, which can only measure flow velocity at a limited set of discrete points and within a limited range of flow angularity.

Particle Image Velocimetry (PIV) is an optical, non-intrusive, laser-based flow measurement technique that quantifies two components of flow velocity with high spatial resolution. To measure a flowfield using PIV, the flow is seeded with micron-sized seed particles and is illuminated by a thin laser sheet. A pair of images is captured in quick succession by a Charged Coupled Device (CCD) camera. The pixel displacement of the illuminated particles in these two images is used to determine the flow velocity. To achieve high spatial resolution of the measurements, the images are divided into a grid of interrogation regions. The particles in an interrogation region from each frame of the image pair are cross-correlated and the identification of a signal peak in the cross-correlation provides an average particle displacement for the region. This measured displacement is divided by the known pulse separation time between the images, resulting in a velocity magnitude and direction. This process is repeated for each region, providing a velocity map for the full image.

Stereo Particle Image Velocimetry (SPIV) is an advanced variant of PIV, allowing all three velocity components to be measured simultaneously. For SPIV, two spatially-separated cameras are used to image the same region in space from two different optical perspectives, as shown in Fig. 1. Because of the difference in optical perspective, the two cameras image the same velocity field with a slightly different image plane. SPIV analysis of the images resolves both in-plane and out-of-plane velocities, providing three velocity components for each interrogation region. The introduction of SPIV as a flow measurement technique will profoundly enhance experimental capability for the SWT. The Naval Innovative Science and Engineering (NISE) program funded this test to demonstrate PIV and SPIV capability in the SWT.

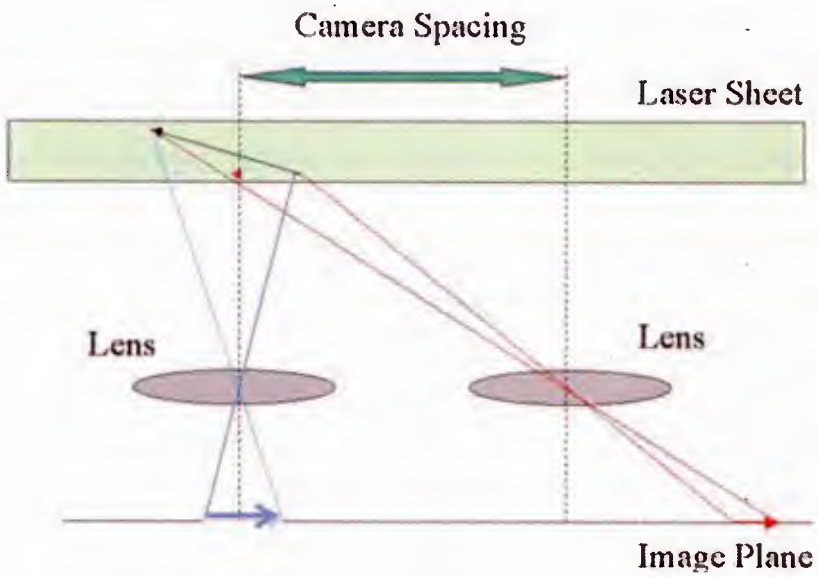

Figure 1. An example of SPIV setup.[1]

The objectives of the test program were as follows:

1) Evaluate the effectiveness of available smoke generation machines for seeding the flow in the SWT with the appropriate size and density of seed particles. Select a smoke machine for use in PIV/SPIV testing and determine a procedure for use of the smoke machine during test execution.

2) Perform PIV and SPIV along the flight deck of a ship model to demonstrate capability of capturing PIV/SPIV data in the wind tunnel.

3) Configure the test setup to capture airwake measurements at test conditions and flowfield locations corresponding to measurements previously taken using multi-sensor fast-response probes.

Accomplishing these objectives allowed the goals for this project to be met, namely; to demonstrate the capability to perform PIV/SPIV experiments in the SWT, to develop wind tunnel SPIV expertise at NSWCCD, and to define the abilities and limitations of performing future SPIV experimentation in the wind tunnel.

The initial test phase evaluated available smoke machines for effectiveness in seeding the flow for SPIV testing. This effort resulted in the selection of smoke generation hardware and development of procedures for its use during testing. The smoke output settings for the machine were tuned in response to the seed escape rate of the tunnel, resulting in instructions for use of the smoke machine to properly seed the flow during subsequent SPIV testing at varying test speeds.

PIV and SPIV testing were performed on an existing generic frigate model (scale of 1:100) in the SWT using expertise and equipment that reside at NSWCCD. The model was mounted on a ground board, which simulated the ocean surface and raised the model above the wind tunnel boundary-layer build-up along the tunnel floor. 2-D PIV data were collected longitudinally along the centerline of the flight deck and along additional planes in the longitudinal direction over the flight deck as well. SPIV was also performed to capture data in these same longitudinal planes. Finally, additional longitudinal planes fore and aft of the flight deck were tested (both with PIV and SPIV data collection) to map the total ship flowfield along the centerline from fore of the bow to aft of the stern. The experimental setup was then reconfigured to capture data in a port-to-starboard (lateral) plane across the flight deck of the model. The location of this plane was mid-way between the hangar and the stern. SPIV measurements were made for the lateral plane.

Measurements across both longitudinal and lateral planes were taken at a model heading of 0 degrees with respect to wind direction (heading into the wind). Initial PIV/SPIV measurements were made at a wind speed of 30 knots, followed by 60 knots and 90 knots. After these initial runs, a test speed of 60 knots was used for the remainder of the test program. Flowfield velocity measurements from SPIV were compared to previously acquired pressure probe velocity measurements from the same test article.

FACILITY

The test facility for this experiment was the NSWCCD 8' x 10' Subsonic Wind Tunnel (SWT). A schematic of the flow circuit of the facility is shown in Fig. 2a. The NSWCCD 8' x 10' SWT is a general purpose, continuous flow, closed circuit facility with a closed jet test section. The wind speed range of the tunnel is from 10 to 275 ft/s (6 to 163 knots) and the test section static pressure is atmospheric. The test section width is 10 ft, height is 8 ft, and length is 14 ft. An exterior photo of the facility is shown in Fig. 2b.

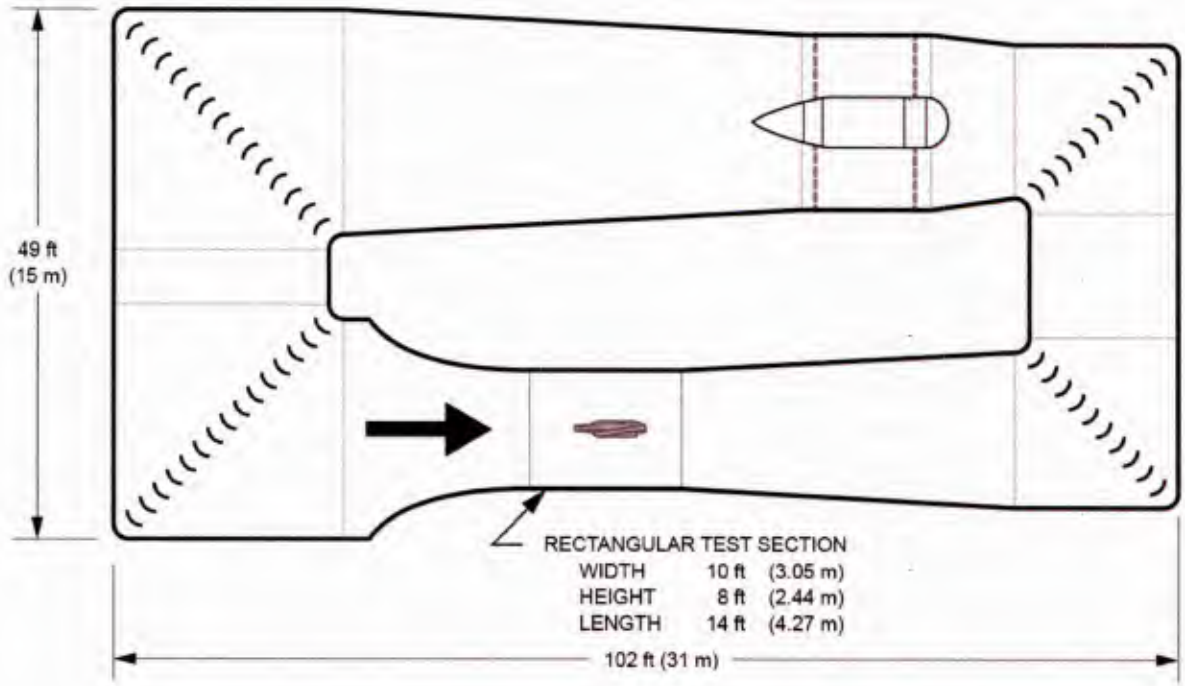

Figure 2a. NSWCCD 8' x 10' Subsonic Wind Tunnel circuit diagram, overhead view.

Figure 2b. NSWCCD 8' x 10' Subsonic Wind Tunnel exterior view.

MODEL, TEST SETUP AND INSTRUMENTATION

Model Description

A ship model with simple geometry was desired for the execution of this test because it allowed for the measurement of aerodynamic flowfield characteristics associated with clean fundamental shapes. The "Simple Frigate Shape 2" (SFS2) geometry was chosen based on its simplified geometry, representative of the fundamental features of an above-waterline frigate. SFS2 is the successor of the SFS1 defined by The Technical Cooperation Panel (TTCP) to compare the results of different experimental and computational methods used across the member nations. The SFS2 geometry has been recently used by researchers in several countries, and features a forward section and triangular bow that was added to the original SFS1 geometry. A schematic of the SFS2 geometry is shown in Fig. 3.

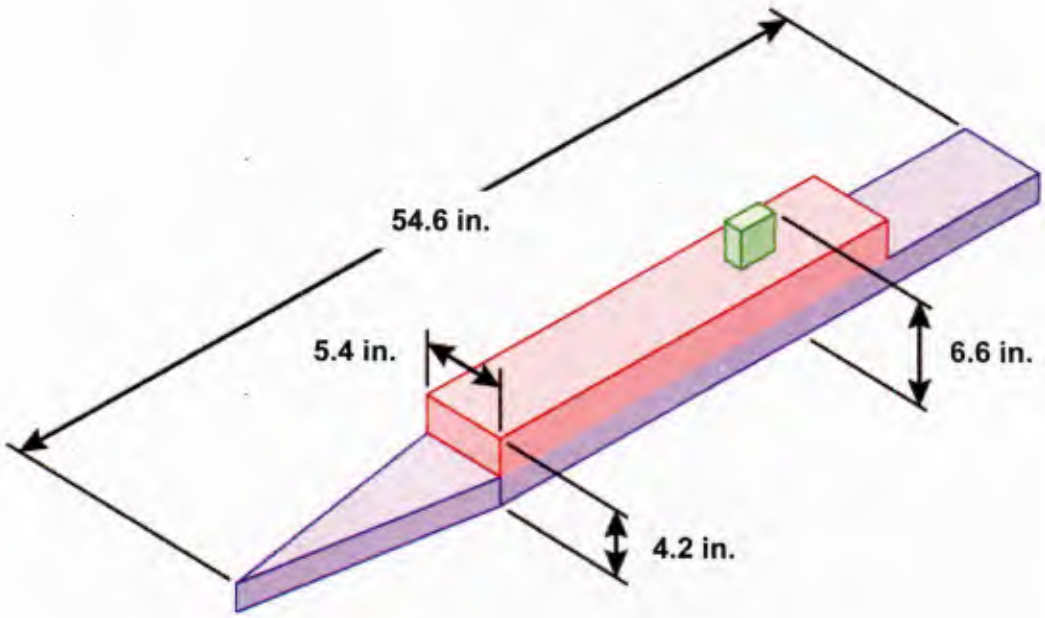

Figure 3. SFS2 schematic showing key model-scale dimensions.

The SFS2 model selected for this test is of 1:100 scale, which corresponds to a length of 4.55 ft. The 1:100 scale model was chosen due to its use in a 2012 test at NSWCCD, during which flowfield measurements were made with Aeroprobe five-hole fast-response velocity probes.[2] This data set provided a unique opportunity for comparison of the previous data with the newly acquired PIV/SPIV velocity data. The model is fabricated from a high-density closed cell foam, and an aluminum mounting plate is attached to the bottom at the mid-length, centerline position. The 1:100 scale test article is shown in Fig. 4.

The model was painted flat black prior to execution of the test to minimize surface laser reflections and to eliminate potential background noise during PIV imaging. The model was modified to mount directly to the ground board (which was also painted flat black) via two aluminum mounting strips. This allowed the model to be moved to attain SPIV measurements in different planes without having to reposition and reset the cameras and optics. In addition to painting the model and ground board flat black, most of the test section light fixtures were

covered with flat black wooden panels and the windows were covered with opaque material to further darken the test section to enhance PIV results. Opaque material was removed from a portion of one window to facilitate camera use. The test installation is shown in Fig. 5.

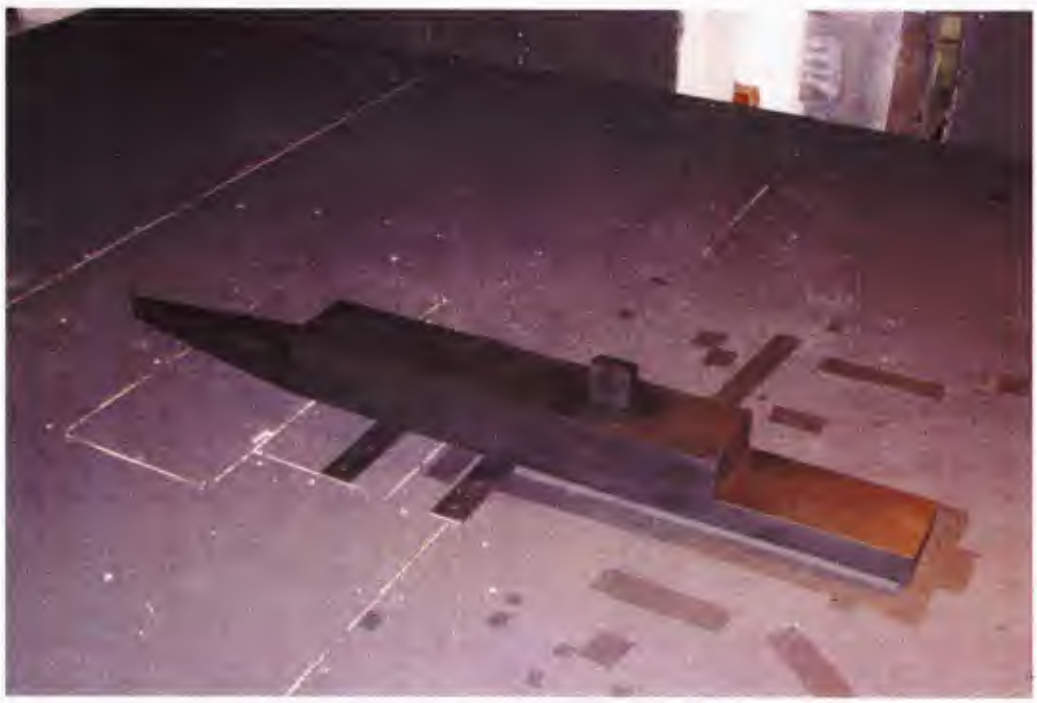

Figure 4. Simple Frigate Shape 2, 1:100 scale model.

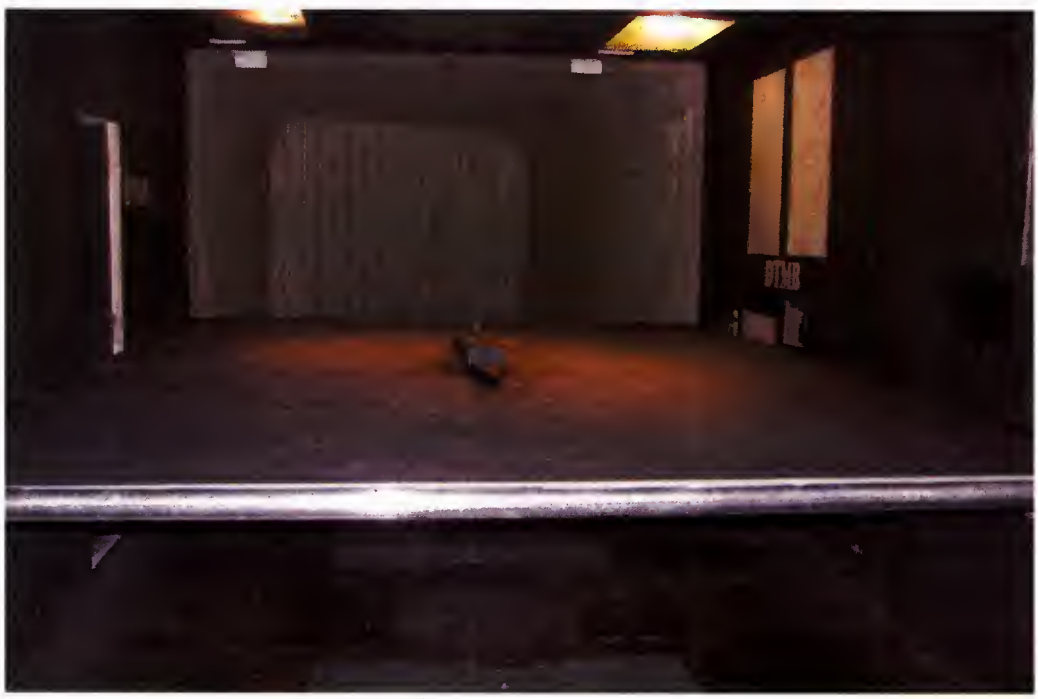

Figure 5. SWT test section with ground board and SFS2 model installed.

Test Setup and Instrumentation

Wind tunnel speed was measured by two pitot probes mounted on opposite tunnel walls upstream of the model and above the ground board. The pitot probes were connected differentially to Scanivalve 1-psi transducers. A secondary measurement of wind tunnel speed was made with the piezometer ring with pressures differentially measured by a Scanivalve 1-psi transducer. The transducers were calibrated using a pressure standard (a Mensor CPG 2500 with 0 to 20 in H_20 range at 4-deg C) with a calibration traceable to national standards. Wind tunnel speed was corrected for model blockage effects and compressibility. A "J-type" thermocouple located behind a fairing on the ceiling of the test section measured tunnel temperature. Barometric pressure was measured by a Mensor DPG II Model 14000B gauge calibrated to national standards.

The data acquisition system was a dual chassis National Instruments (NI) cDAQ-9178 compact DAQ (Ethernet version) sampling at 2000 Hz. The cDAQ has multiple modules installed to handle input from specific types of data channels. The installed modules are as follows:

1) NI 9237 "4 channel, 24-bit half/full bridge analog input module", quantity – 4
2) NI 9213 "thermocouple input module, 16-channel", quantity – 1
3) NI 9239 "+/-60/+/-10 V, 24-bit simultaneous, channel-to-channel isolated analog input module, 4-channel", quantity – 3
4) NI 9401 "high-speed, bidirectional digital I/O module, 2 channel", quantity 1

The NI 9237 modules received input from the pressure transducers. The NI 9213 interfaced with the tunnel temperature thermocouple. The NI 9239 and the NI 9401 were not used during this test. A channel list of test instrumentation is shown in Table 1.

Table 1. Instrumentation Listing.

No.	Description	Instrument	Manf.	Model	Range
1	Tunnel Vel (south pitot)	Transducer	Scanivalve	CR24D	1 psi
2	Tunnel Vel (north pitot)	Transducer	Scanivalve	CR24D	1 psi
3	Tunnel Vel (piezo)	Transducer	Scanivalve	CR24D	1 psi
4	Total P (north pitot)	Transducer	Scanivalve	CR24D	1 psi
5	Tunnel Temperature	Thermocouple	Omega		1620 °F
6	Barometric Pressure	Abs Pressure	Mensor	DPG II	17 psia

Two different smoke generators were used during an initial testing phase at zero wind velocity. These are the TSI 9307 single jet oil droplet generator using olive oil (Fig. 6a), and the Aerolab smoke generator using propylene glycol (Fig. 6b). After this initial test, it was determined that the TSI device produced particles that would last in the freestream longer and would therefore be used for seeding during the test program. The Aerolab device would serve as a backup.

Figure 6a. TSI 9307 oil droplet generator.

Figure 6b. Aerolab smoke generator system.

A PIV/SPIV system was used to acquire velocity measurements of the flowfield around the model. The system used two Big Sky Nd:YAG lasers, which can fire at 200 mJ per pulse. The lasers were operating at 150 mJ. Each laser fired at 3.0 Hz, with offsets between firing of laser one and laser two set to Δt = 25 to 90 μ s during the test. The cameras were Pulnix model TM-4200CL featuring a CCD array of 2048 x 2048 pixels (4.19 megapixels). The data from the cameras were acquired by a Boulder Imaging computer model Quazar 2.0 with a frame grabber.

For the test setup, the laser system and its accompanying optics were mounted to a secure breadboard. The breadboard was clamped to the top of the wind tunnel. This setup allowed the laser sheet to illuminate the test section through an opening in the ceiling of the wind tunnel. A schematic of this set-up is shown in Fig. 7. A black plastic tent structure was constructed which enclosed the laser system atop the tunnel, preventing any laser light from escaping into the surrounding area. Air conditioning was vented to the tent to keep equipment in the tent cool, as well as for the safety and comfort of personnel. Black plastic material draped portions of the side of the test section to prevent light transfer through the open slots in the test section walls.

Three cameras were positioned outside the wind tunnel. For 2-D PIV in the longitudinal plane, a camera with a 105 mm lens was mounted to a tripod and oriented orthogonally to the light sheet, just outside of the main wind tunnel door on the south side of the test section. This resulted in a 9.25 in. by 9.25 in. region of interrogation (ROI). For SPIV, two cameras with 135 mm lenses were mounted inside the side wall gaps (slots) of the tunnel and captured images for both the longitudinal and lateral planes (Fig. 8). This arrangement kept the two SPIV cameras outside of the tunnel flow. The SPIV cameras produced a 15 in. wide by 6.25 in. high ROI. For each of the two planes, i.e. the lateral and longitudinal planes, the SPIV lenses were angled non-orthogonally to the CCD using a Scheimflug adaptor to achieve sufficient image focus. A schematic showing notional camera placement for PIV/SPIV measurements in the longitudinal and lateral planes is shown in Fig. 9. An illustration of the PIV/SPIV installation in the test section is shown in Fig. 10.

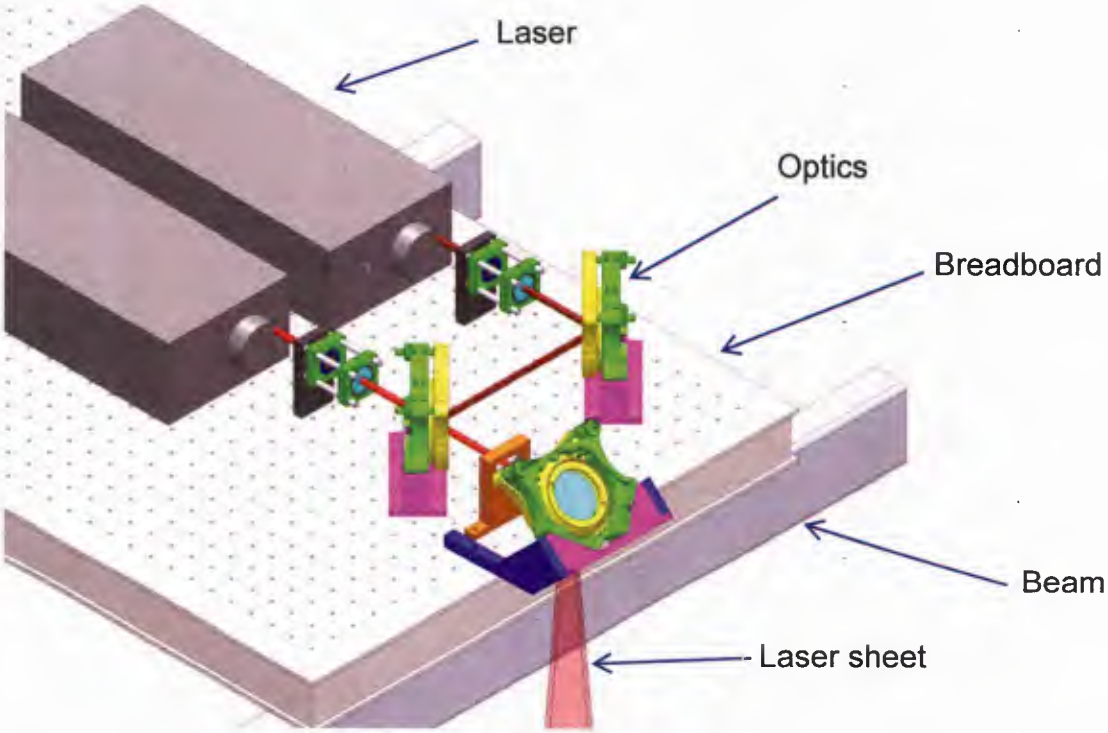

Figure 7. Laser system and optics mounted above the wind tunnel test section.

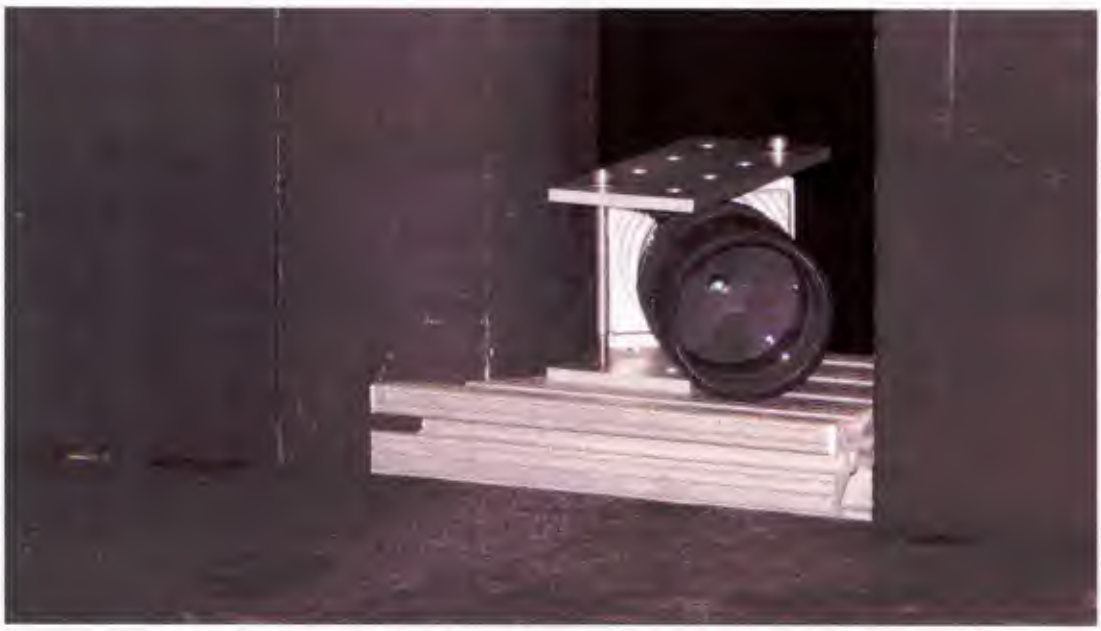

Figure 8. Pulnix camera mounted in the tunnel side wall slot, angled upstream.

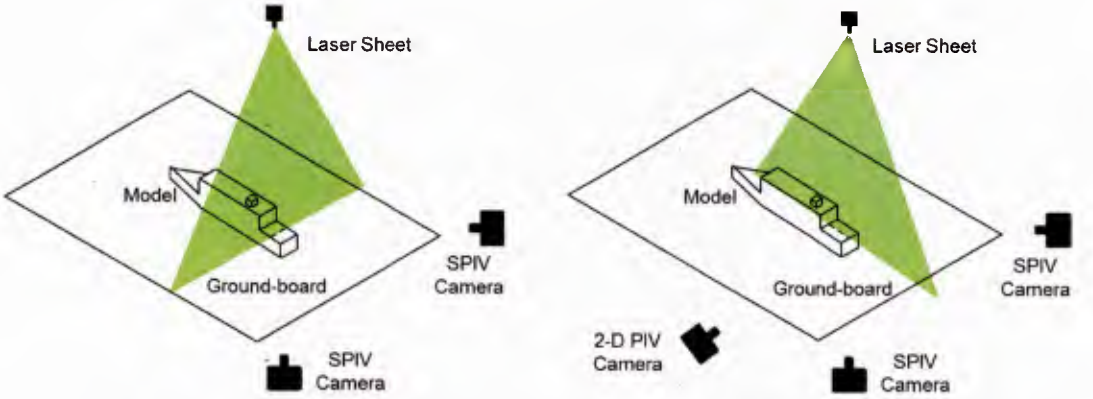

Figure 9. Schematic of notional PIV/SPIV measurement planes and camera placement (left – lateral plane at mid-flight deck, right – longitudinal plane at ship centerline).

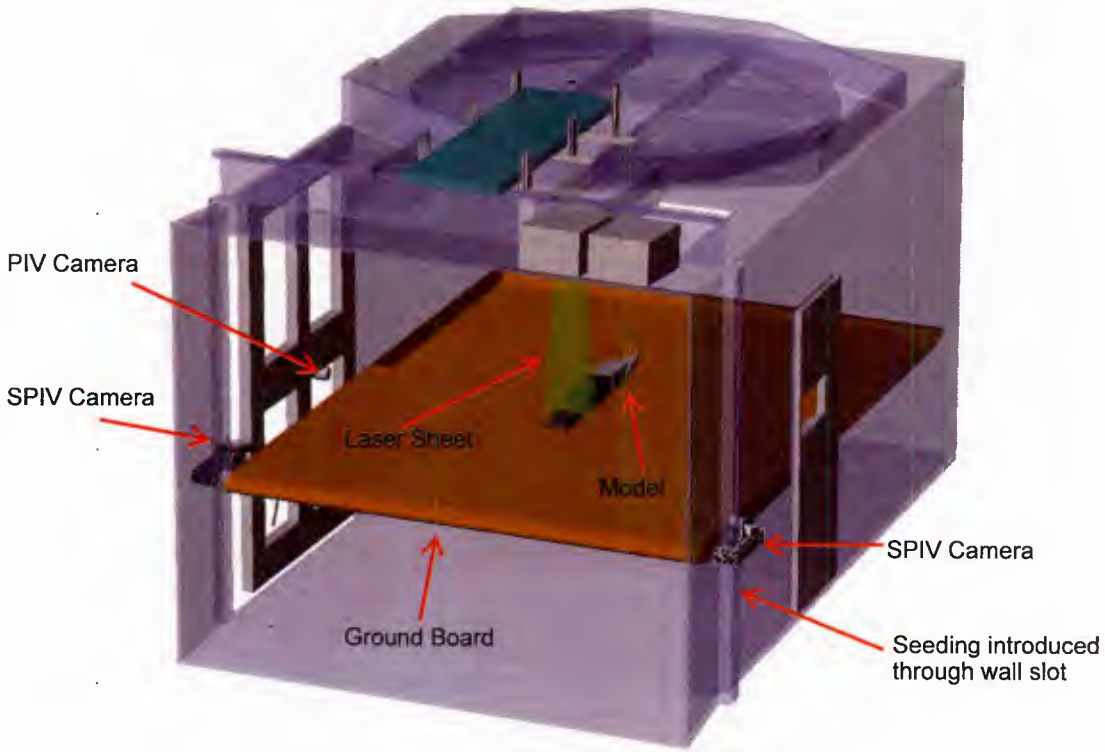

Figure 10. Test section showing PIV and SPIV installation.

TEST PROCEDURE

The model was installed at a 0-deg heading (head winds) for the entire test. The test program commenced with testing and alignment of the laser system, and calibration of the PIV/SPIV camera systems. A two-sided vendor supplied calibration plate positioned above the model flight deck was used during the calibration process (Fig. 11). Initial wind-on testing was dedicated to seeding optimization, and PIV testing in the bow-stern (longitudinal) plane along the ship centerline at a heading of 0 degrees and windspeeds of 30, 60, and 90 knots. Laser Δt settings nominally ranging from Δt = 25 to 90 μ s were used to determine the appropriate time between laser pulse firings to achieve well-correlated results. Seeding was introduced when the tunnel was at minimum or "idle" speed, and was adjusted throughout the run to maintain proper seeding density. Seeding was fed into the test section via a tube through the slot in the north test section wall, as indicated in Fig. 10.

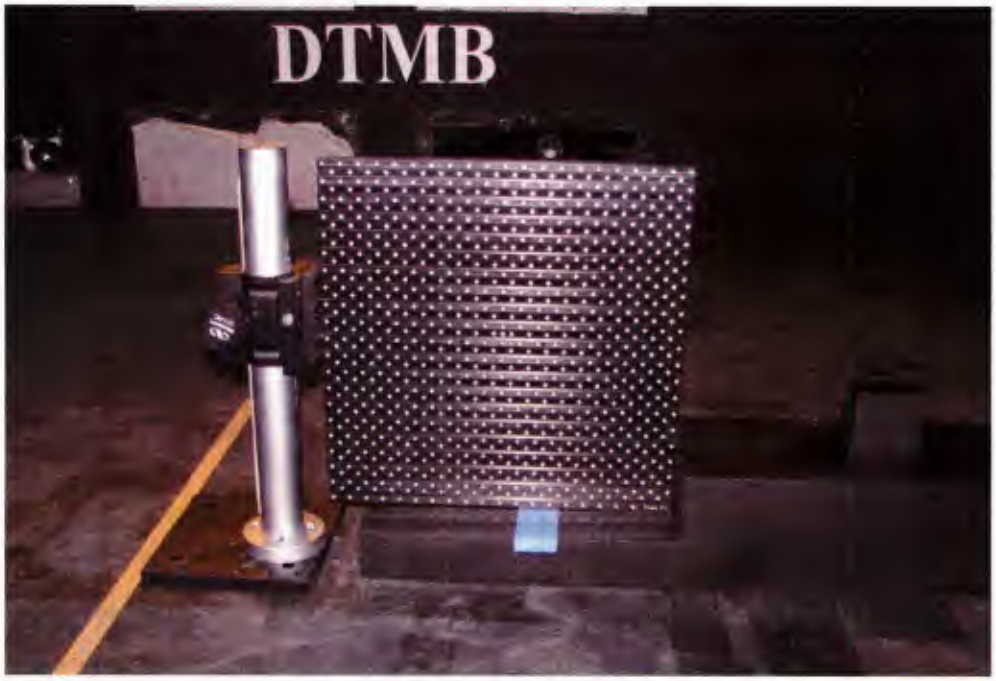

Figure 11. Two-sided calibration plate mounted above the model flight deck.

After collecting PIV (2-D) measurements, the data acquisition system was reconfigured to acquire data from the SPIV cameras to get SPIV measurements at these same conditions. PIV and SPIV measurements were also made without the model in the tunnel to measure freestream flow over the ground board (to establish a "baseline" flow measurement). Following centerline measurements, PIV and SPIV measurements were taken at additional longitudinal planes over the flight deck, some of which matched with four previous velocity probe vertical survey data locations, at a windspeed of 60 knots (Fig. 12a). Note that definitions of the coordinate system for the test are contained in Fig. 12, and that x, y, and z coordinates are non-dimensionalized by H, the height of the hangar above the flight deck (2.4 in.). Additional planes were captured by moving the ship model and reattaching it to the ground board. This resulted in repositioning the laser sheet over a different portion of the test article while not moving the lasers or cameras or affecting system alignment or settings. Data quality was assessed before moving from one plane to the next.

After completing longitudinal plane measurements over the flight deck, the model was incrementally moved fore and aft to acquire PIV/SPIV measurements along the ship centerline above all other regions of the ship, from fore of the bow to aft of the stern (Fig. 12b). This allowed for PIV/SPIV results to be "stitched" together to get a measurement set of the complete ship flowfield along the centerline.

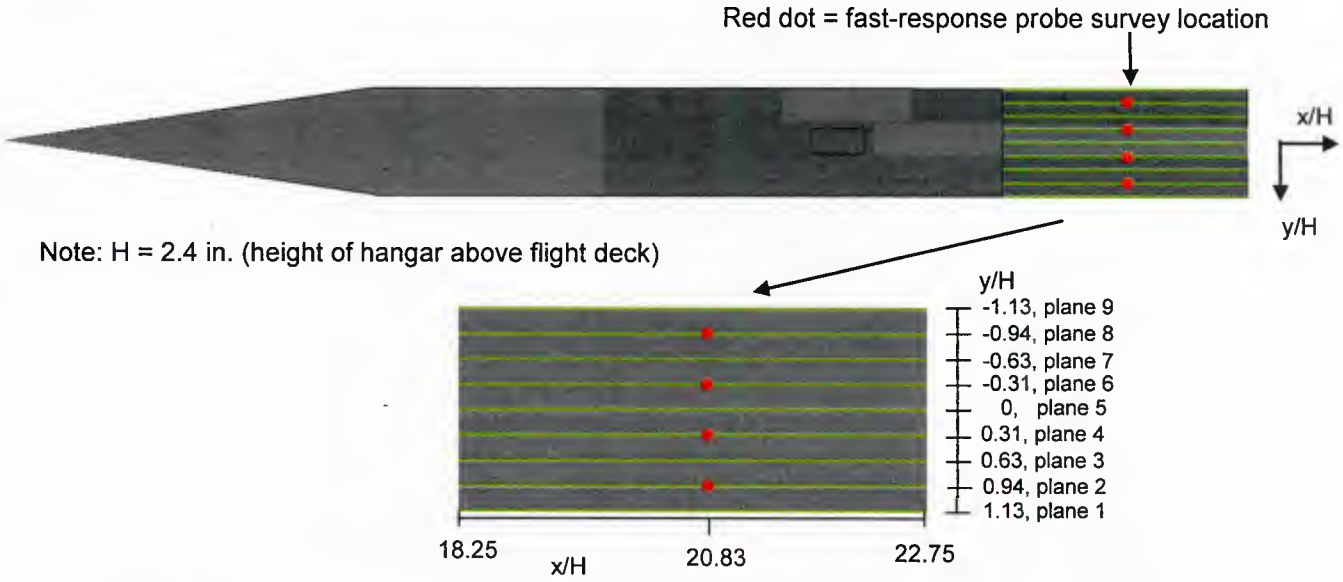

Figure 12a. Nine longitudinal PIV/SPIV planes on the flight deck and corresponding four velocity probe survey locations, with enlarged view for detail.

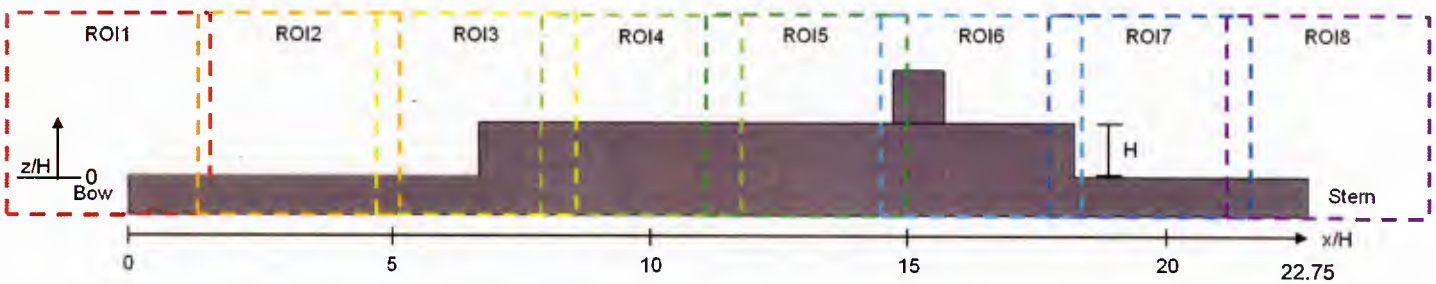

Figure 12b. Eight ROI's for PIV/SPIV measurements along the model centerline.

For the final phase of the test program, the camera and laser system were reoriented for the shift to port-starboard (lateral) plane SPIV measurements at 60 knots. No 2-D PIV measurements were attempted for the lateral plane. The final wind-on testing was dedicated to a lateral plane that was half-way between the hangar and the stern on the flight deck (x/ H = 20.5, or 5.4 in. from the stern). Figure 13 shows the lateral plane, viewed from the stern looking upstream. Figure 14 shows a photo of the laser sheet with seeding to illustrate the lateral plane setup.

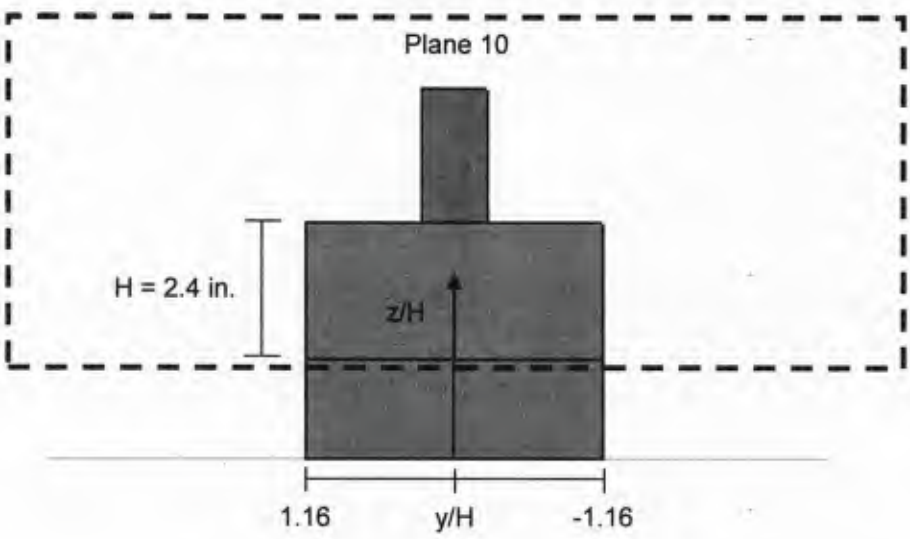

Figure 13. SPIV lateral plane over the flight deck, midway between the hangar and the stern.

Figure 14. Photo showing lateral plane laser sheet with flow seeding (no substantial flow in the tunnel, for illustrative purposes only).

During the test, 500 image pairs were collected per camera and per test point, corresponding to 500 image pairs for PIV data acquisition, and 500 image sets for SPIV data acquisition. Variations of Δt and the analysis of PIV/SPIV data for each Δt setting resulted in selection of the optimal Δt settings for the remainder of the test program as follows: a Δt setting

of 40 μs was selected for the longitudinal PIV and SPIV testing at 60 knots, and a setting of 25 μs was selected for the lateral plane SPIV testing at 60 knots. Nine longitudinal planes over the flight deck and one lateral plane were measured. The complete test matrix is shown in Table 2, with planes numbered as per Figs. 12 - 13.

Table 2. PIV/SPIV Test Matrix.

Model	Velocity (knots)	Heading	Technique	Plane
No Model	30, 60	N/A	PIV	Longitudinal, plane 5 (centerline)
No Model	30, 60	N/A	SPIV	Longitudinal, plane 5 (centerline)
1:100	30, 60, 90	0 deg	PIV	Longitudinal, plane 5 (centerline)
1:100	30, 60, 90	0 deg	SPIV	Longitudinal, plane 5 (centerline)
1:100	60	0 deg	PIV	Longitudinal, planes 1, 2, 3, 4, 6, 7, 8, 9
1:100	60	0 deg	SPIV	Longitudinal, planes 1, 2, 3, 4, 6, 7, 8, 9
1:100	60	0 deg	PIV	Longitudinal, CL, ROI's 1, 2, 3, 4, 5, 6, 8 (ROI 7 = plane 5)
1:100	60	0 deg	SPIV	Longitudinal, CL, ROI's 1, 2, 3, 4, 5, 6, 8 (ROI 7 = plane 5)
1:100	60	0 deg	SPIV	Lateral, plane 10

RESULTS

This test effort was performed to demonstrate the ability of the PIV/SPIV system to collect flowfield velocity measurements over a range of tunnel speeds, for longitudinal and lateral planes, to define the abilities and limitations of performing future SPIV experimentation in the wind tunnel, and to study and measure as much of the model airwake as time permitted. An example of a raw PIV image (zoomed in) is shown in Fig. 15, which highlights a typical concentration of flow seeding particles.

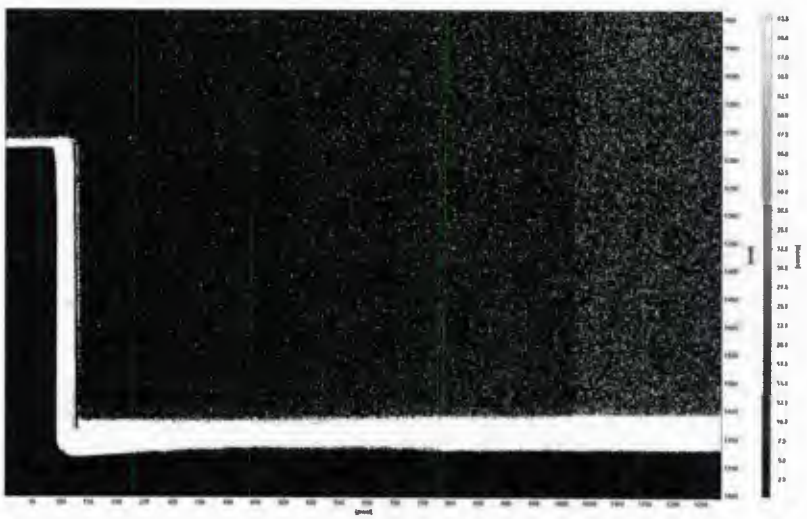

Figure 15. Raw PIV image showing flow seeding over the flight deck.

All results presented correspond to a 0 deg ship heading and a wind tunnel speed of 60 knots (30.9 m/s). Some test results are compared to previous fast-response velocity probe measurements.[2] The test was designed to demonstrate PIV/SPIV capability in the SWT using a simplified ship geometry. As can be seen in the results in this section, PIV/SPIV measurements successfully revealed the flow features that were expected above and behind this simple geometry.

Early in the test, measurements of freestream velocity over the ground board with no model present were made to verify the functionality of the PIV/SPIV setup. Initial PIV/SPIV results indicated a freestream velocity over the ground board of approximately 56 knots, while the tunnel pitot probes indicated a freestream velocity of nominally 60 knots. This discrepancy was greater than expected given the recent calibration of the wind tunnel pitot probe pressure transducers, and the high accuracy typically associated with PIV/SPIV techniques. Potential causes for the discrepancy were discussed. A light sensing diode was used to test the accuracy of the triggering of the laser system during PIV/SPIV data acquisition. Using this device, it was discovered that a lag existed between triggering of the lasers and actual laser firing. Since the lag was different in each of the two lasers, the resulting Δt, or time gap between laser pulses from the first laser and the second laser, was smaller than the selected setting value by approximately 3.4 μ s. The Δt that was measured by the light sensing diode was used to correct the PIV/SPIV freestream data, which resulted in freestream velocities of 60 - 61 knots, which agreed well with pitot probe measurements. This correction to Δt was applied to all of the test data as a post-processing step.

To better understand the steady-state and large-scale flow features within the airwake, Fig.16 shows the average flowfield (based on averaging all image pairs) over the topside of the ship as contours of velocity magnitude normalized by the freestream velocity. These results are produced by time-averaging the two-dimensional PIV velocity measurements in each ROI and stitching ROI's 1-8 together (ROI's 1-8 as defined in Fig. 12b). Blue regions indicate slower or reversed flow, while red is faster flow. In general, the superstructure of the ship induces large regions of flow separation and turbulence. The stack, hangar, and stern all form rearward facing steps, which cause the flow to separate off of the edges and form large recirculation regions. A close-up of the aft end of the ship, showing flow streamlines more clearly, illustrates the flow separation in Fig. 17.

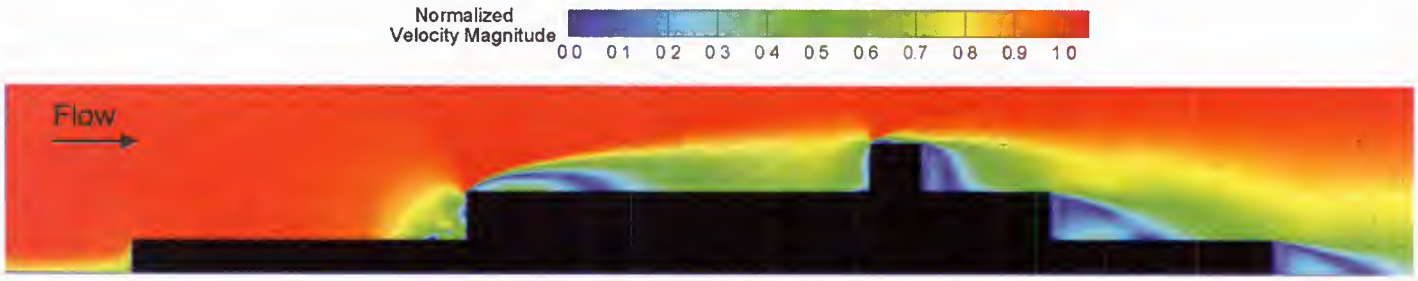

Figure 16. Complete time-averaged PIV flowfield along the model centerline.

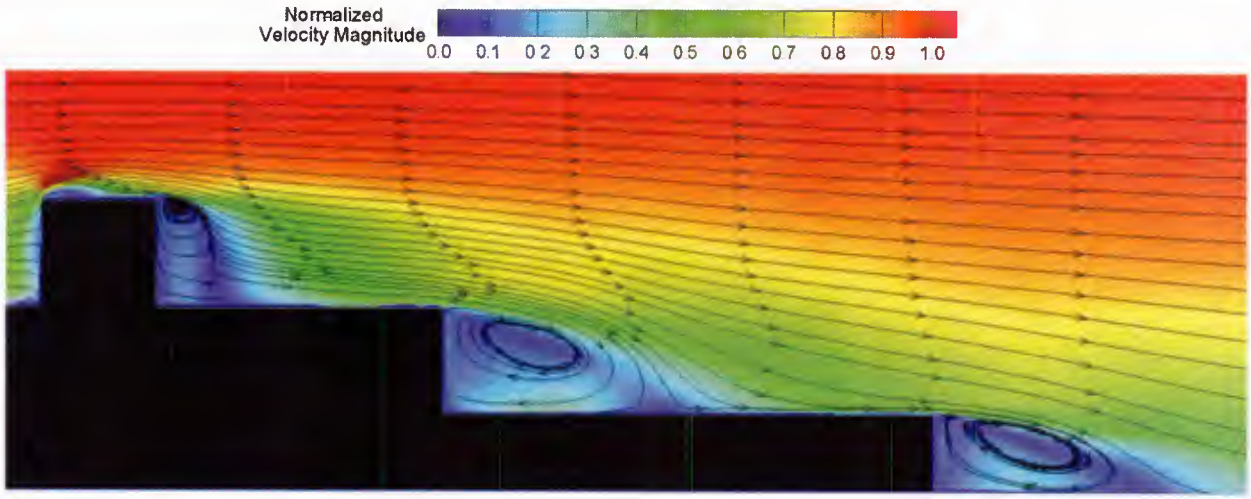

Figure 17. Flow streamlines of time-averaged PIV data over the aft end of the model along the model centerline.

Of particular interest is the flow over the flight deck, just downstream of the hangar (ROI 7). Figure 18 shows a more detailed view of this region. The velocity deficit created by the superstructure extends above the height of the ship, up to z/H ≈ 2.5. Closer to the ship, the flow clearly separates at the edge of the hangar and deflects downward, reattaching at a location of x/H ≈ 21.2. Between the reattachment point and the hangar, there is a region of the airwake with relatively lower velocity magnitude that is recirculating back towards the hangar.

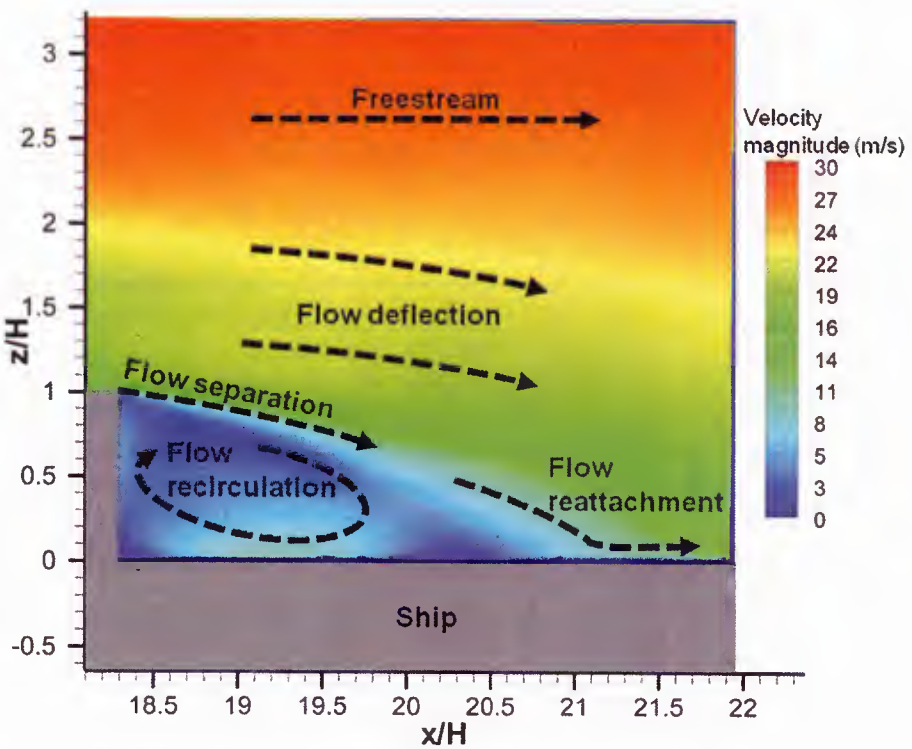

Figure 18. Flow features over the flight deck (centerline) from time-averaged PIV.

The instantaneous velocity field over the hangar reveals a turbulent flow environment. Figure 19a shows a representative instantaneous flow data sample in ROI 7 as contours of normalized velocity magnitude. The flow forms a large vortical region (blue region behind the hangar), which detaches from the hangar and rapidly diffuses as it convects downstream.

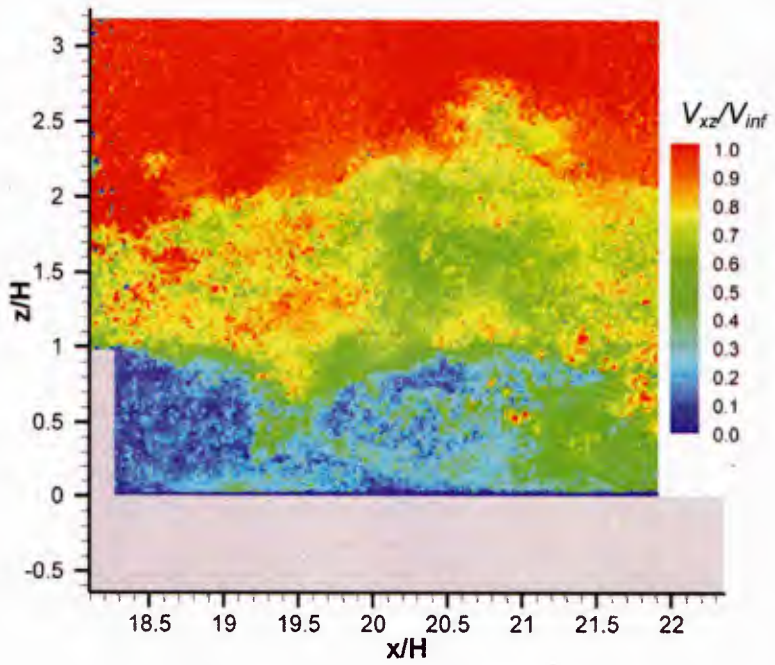

Figure 19a. Contours of instantaneous normalized velocity magnitude over the flight deck.

To better identify the vortical structures in the flow, it was useful to isolate the fluctuating components of velocity at each spatial location. This was done by subtracting the average velocity field from the instantaneous velocity field and running the measurements through a spatial low pass filter. Figure 19b shows the results of this process (using the same data sample from Fig. 19a) as contours of instantaneous vorticity, where blue indicates a clockwise spin and red indicates a counter-clockwise spin. Notice that there is a concentration of higher vorticity just above the flight deck. These regions of vorticity, as well as the shedding of the recirculating region, may induce counter vorticity, resulting in a turbulent flow environment. The results also indicate that there are high levels of less coherent vorticity well above the hangar and the stack height.

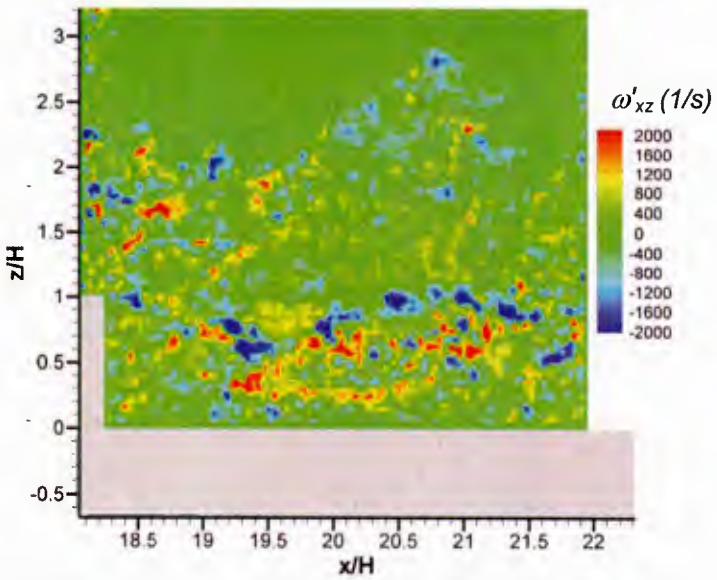

Figure 19b. Contours of instantaneous vorticity over the flight deck.

These less coherent vortical regions have convected from further upstream (i.e., from the stack and the forward step). The instantaneous flowfield just downstream of the stack is shown in Figs. 20a and 20b as contours of normalized velocity magnitude and vorticity, respectively (ROI 6). Flow separation occurred at the forward and rearward edges of the stack, resulting in the production of concentrated vorticity as well as a recirculating region downstream of the stack. These regions of vorticity diffuse as they convect downstream, but are still of significant strength when they are above the flight deck. It should be noted that there is a region of low velocity well above the stack height in Fig. 20a (at x/H ≈ 17.5). The height at which this perturbation occurs in the velocity field suggests that it did not originate at the stack, but rather further upstream.

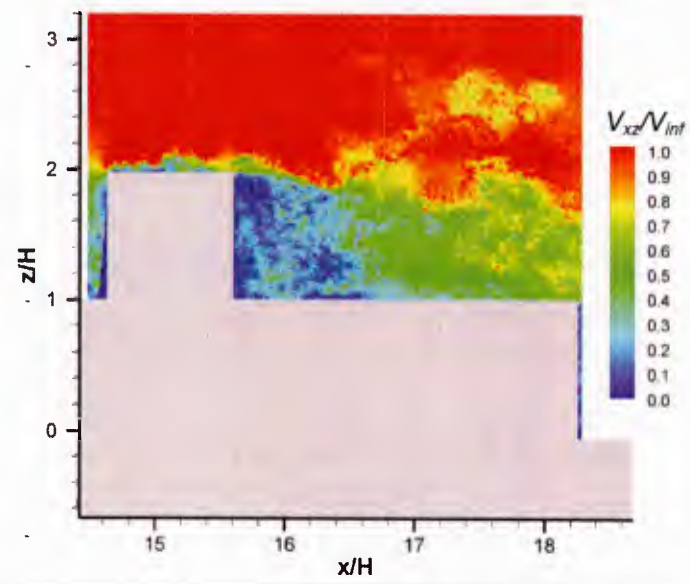

Figure 20a. Contours of instantaneous normalized velocity magnitude downstream of the stack.

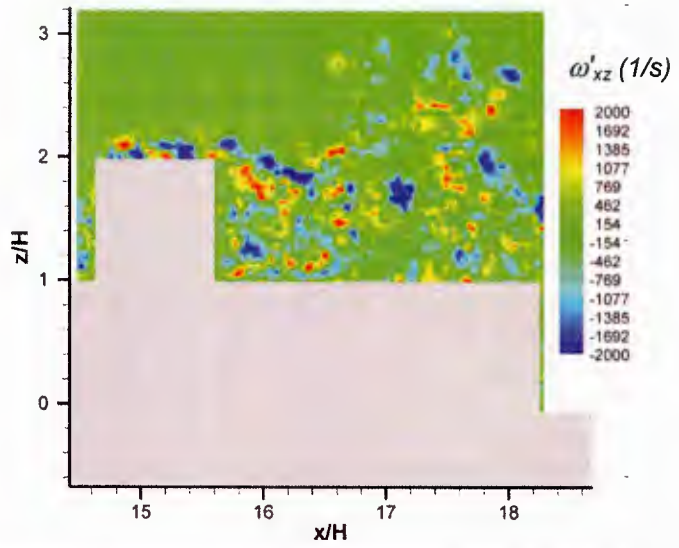

Figure 20b. Contours of instantaneous vorticity downstream of the stack.

To investigate this phenomenon, Figs. 21a and 21b show the flow around the forward step created by the forward face of the superstructure (ROI 3) as contours of normalized velocity magnitude and vorticity, respectively, for a representative instantaneous data sample. In this case, the average velocity was not subtracted from the instantaneous flow velocity in the vorticity calculation. At the edge of the step, the flow separates, again forming a shear layer and a recirculating region; see Fig. 21a. However, Fig. 21b indicates that the shear layer rolls up into vortical regions that are significantly stronger than those produced by the stack or by the rearward step. Even though these vortical regions diffuse, their relatively higher levels of vorticity may allow many of them to persist much further downstream. Those that diffuse rapidly degenerate into turbulence, which still convects towards the stern of the ship, and is likely the reason that the airwake boundary of the ship is well above the stack height. Also notice that there is a thin region of counter vorticity (colored red in Fig. 21b) adjacent to the top edge of the step. This counter vorticity is the presence of a boundary layer that forms on the surface of the ship due to the flow recirculating downstream of the forward step.

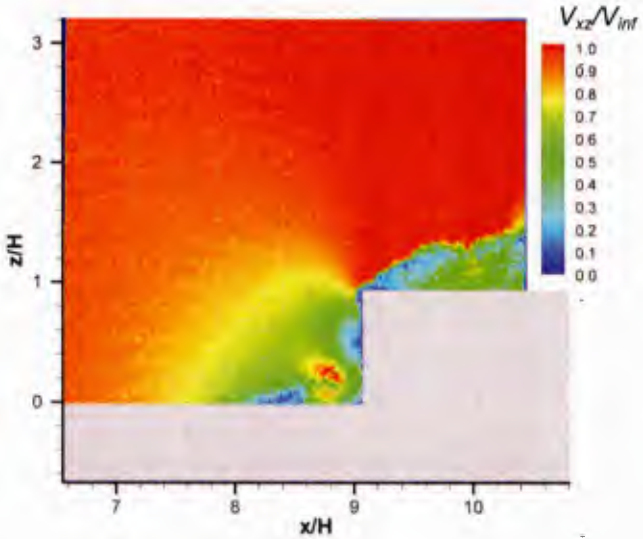

Figure 21a. Contours of instantaneous normalized velocity magnitude at the forward step.

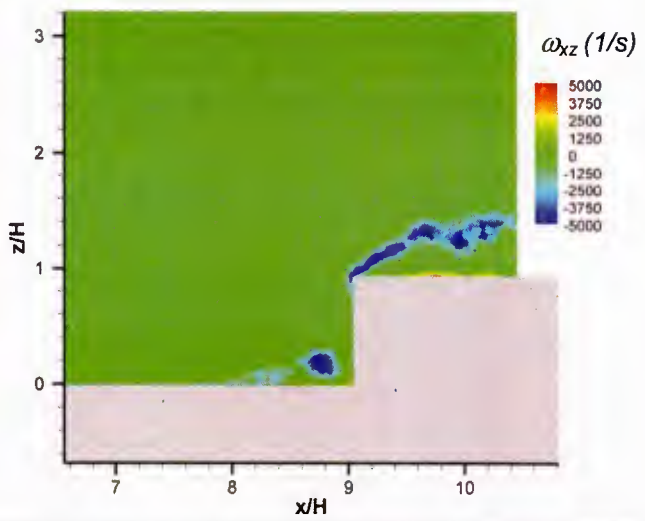

Figure 21b. Contours of instantaneous vorticity at the forward step.

Figure 21b reveals a vortex that forms just upstream of the forward step. The freestream flow impinges on the vertical surface of the forward step, causing the formation of a stagnation point. Below this stagnation point, the flow convects along the surface of the ship and back toward the freestream. Ultimately, the recirculating flow is overpowered by the freestream flow, creating another stagnation point on the horizontal surface, the result being a vortex between the two stagnation points. The vortex is also seen in the time-averaged contours of vorticity in Fig. 21c. It is interesting to note that at non-zero headings such as 60 and 90 deg the whole side of the ship would form a corner with the ground board. It is possible that a vortex would form along the entire side of the ship, introducing a low pressure aerodynamic phenomenon that could affect wind loads measurements on the ship.

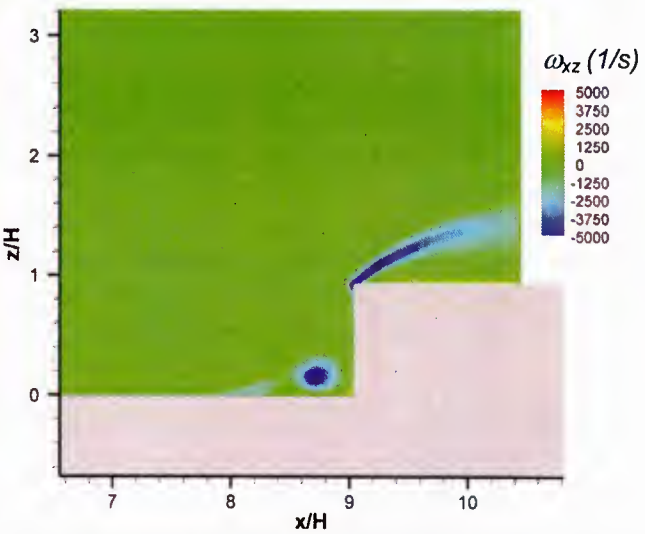

Figure 21c. Contours of time-averaged vorticity at the forward step.

The airwake produced by the superstructure of the ship is also three-dimensional. This three-dimensionality is clearly seen in the SPIV measurements taken at the mid-deck location in the lateral plane (plane 10). Figure 22 shows the results as background contours of the time-averaged *u* component of velocity (out of plane) and vectors of the time-averaged *v* and *w*

components of velocity (every 10th vector is shown to avoid image congestion). Notice that even though the ship is symmetric along its longitudinal centerline, the flow is clearly asymmetric. Though computational studies support this asymmetric flow finding,[3] further study is required to determine the nature of the flow asymmetry. While the out of plane velocity (*u)* is the dominant component of velocity, the other two components (*v* and *w)* are of significant magnitude, with the flow convecting toward the flight deck and then outward, indicating the formation of vortices on the flight deck.

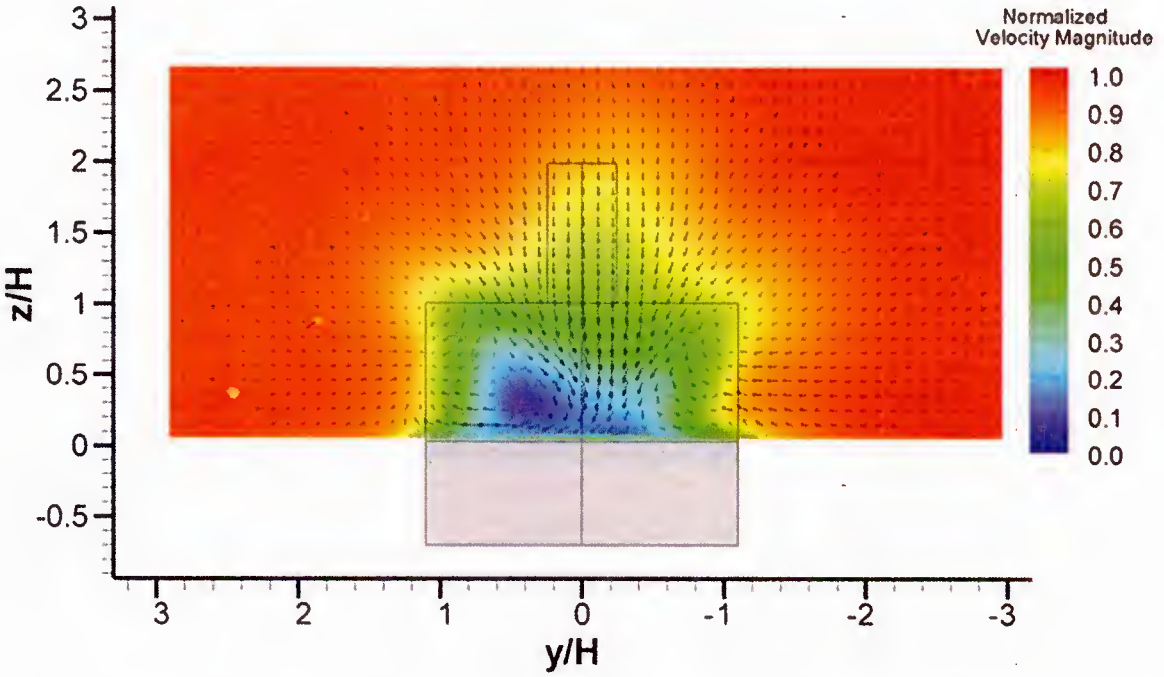

Figure 22. Lateral plane (plane 10, mid flight deck) time-averaged SPIV results.

A lateral survey of the flowfield over the flight deck can be constructed using the longitudinal plane PIV data. The results are shown in Figs. 23 and 24. Figures 23a - 23d show contours of normalized velocity magnitude in planes at y/H = 0.94, 0.31, -0.31, and -0.94. Figures 23a - 23d also compare the fast-response velocity probe (FRP) data (from a previous test)[2] to PIV velocity profiles obtained at the same locations at x/H = 20.83. The plots of the probe data used only the u and w components of velocity to be consistent with the two component velocity content of the PIV data. The results show that there is good agreement between the velocity probes and the PIV measurements. The agreement is better for the two inboard stations (y/H = 0.31 and -0.31) than for the two more outboard stations (y/H = 0.94 and -0.94). Both systems identified a lateral asymmetry in the flow over the flight deck, with the starboard side of the ship inducing higher velocity magnitudes. Moving outward from the centerline of the ship, the recirculation region decreases in size, and the reattachment point moves closer to the hangar. This is also evident in Fig. 24, which shows data from planes 2-9 superimposed on a three-dimensional rendering of the model and flight deck (plane 1 is left off so as not to obscure the other planes behind it).

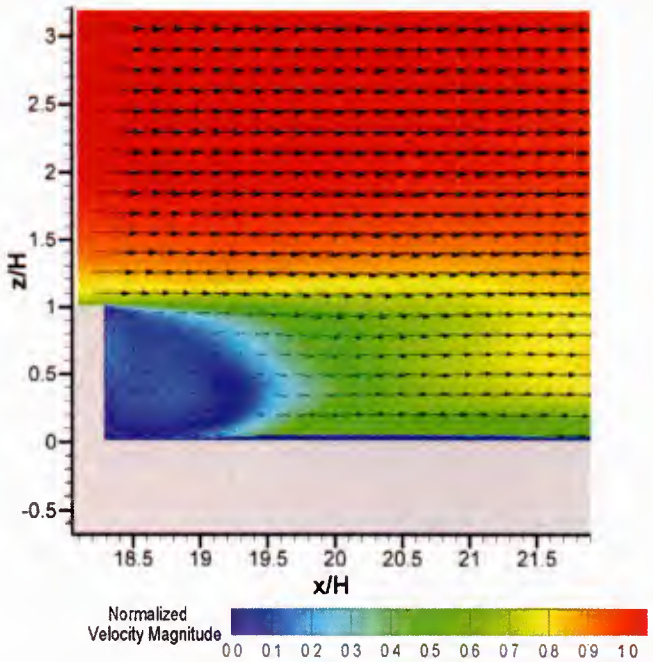

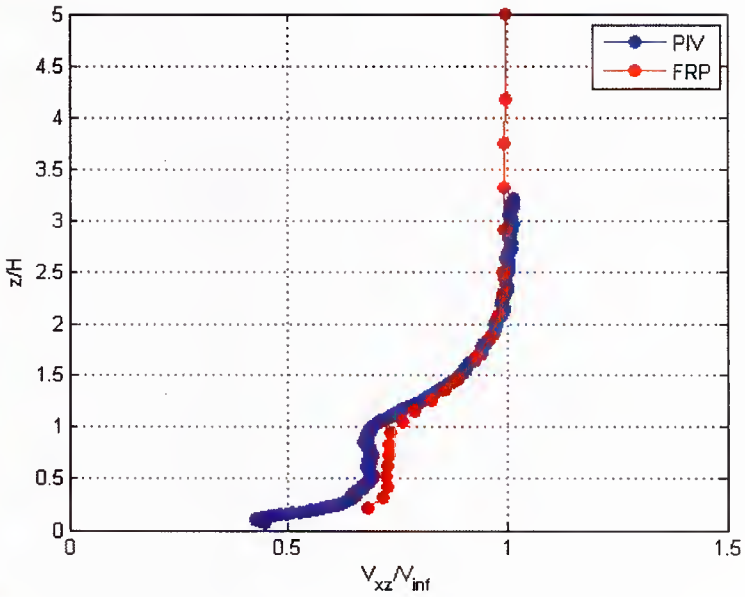

y/H = 0.94

Figure 23a. Contour plot of time-averaged longitudinal plane PIV data (plane 2, y/H = 0.94) and a plot of PIV data and velocity probe data plotted together for y/H = 0.94 and x/H = 20.83.

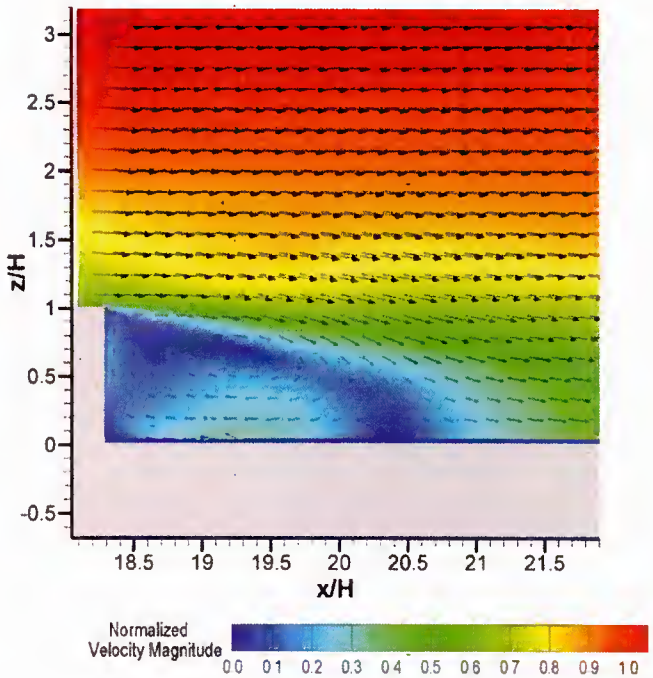

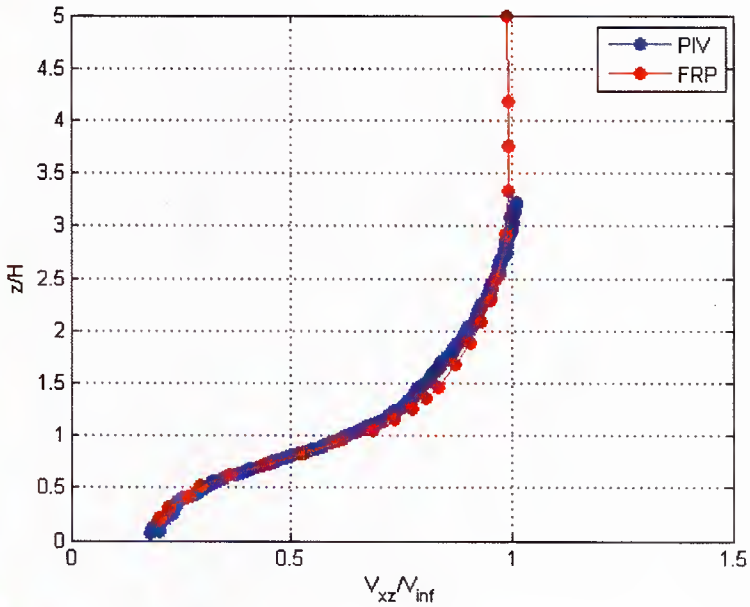

y/H = 0.31

Figure 23b. Contour plot of time-averaged longitudinal plane PIV data (plane 4, y/H = 0.31) and a plot of PIV data and velocity probe data plotted together for y/H = 0.31 and x/H = 20.83.

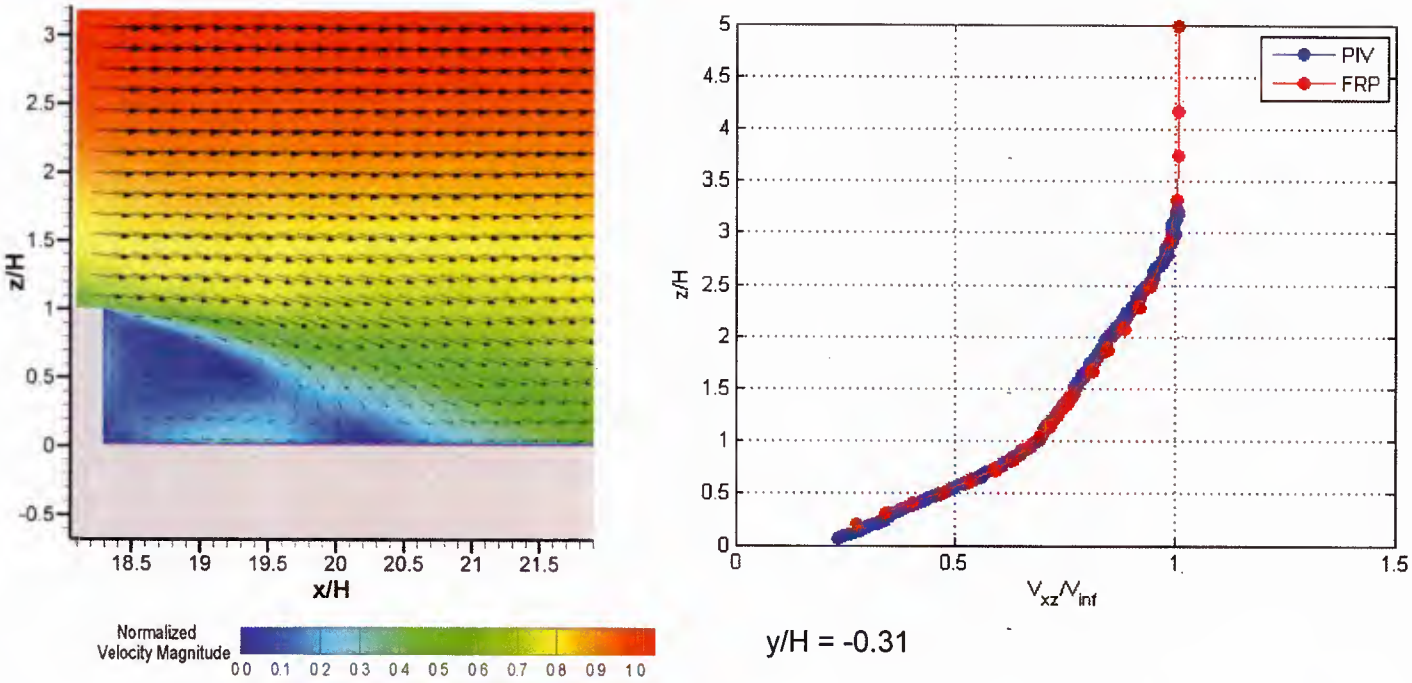

Figure 23c. Contour plot of time-averaged longitudinal plane PIV data (plane 6, y/H = -0.31) and a plot of PIV data and velocity probe data plotted together for y/H = -0.31 and x/H = 20.83.

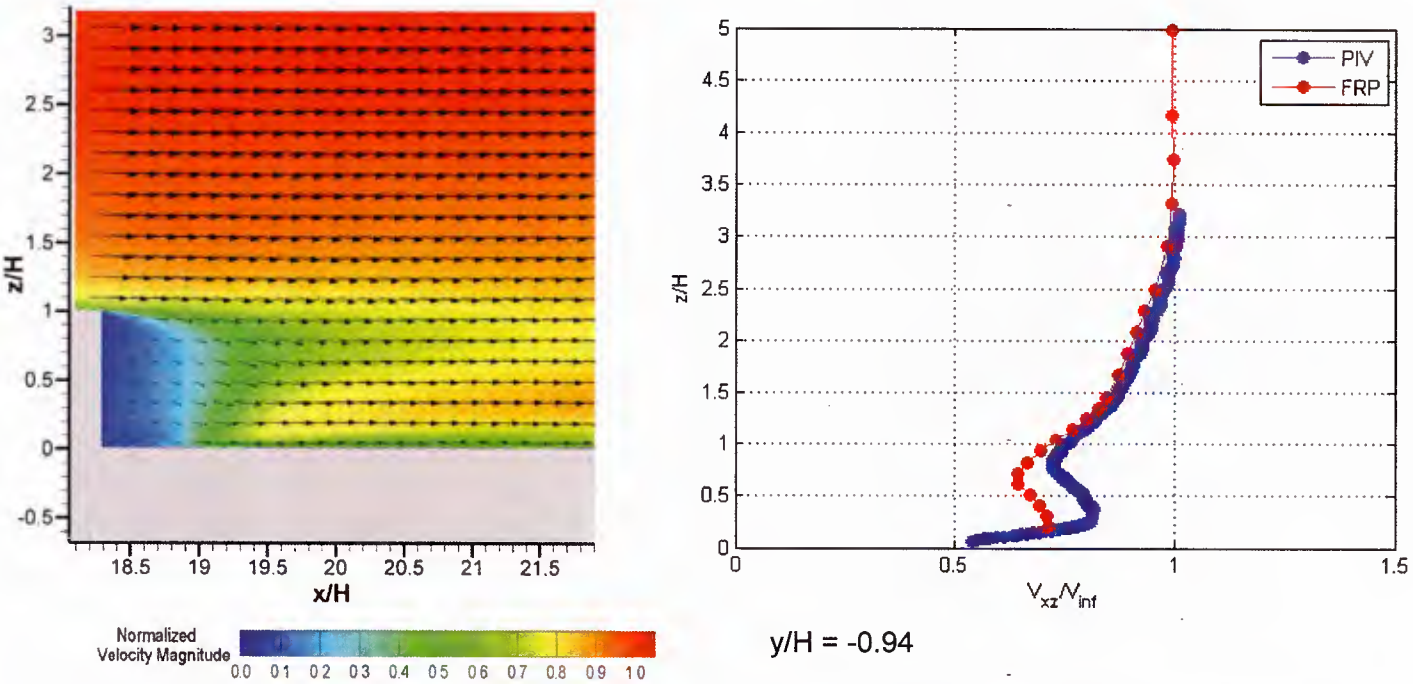

Figure 23d. Contour plot of time-averaged longitudinal plane PIV data (plane 8, y/H = -0.94) and a plot of PIV data and velocity probe data plotted together for y/H = -0.94 and x/H = 20.83.

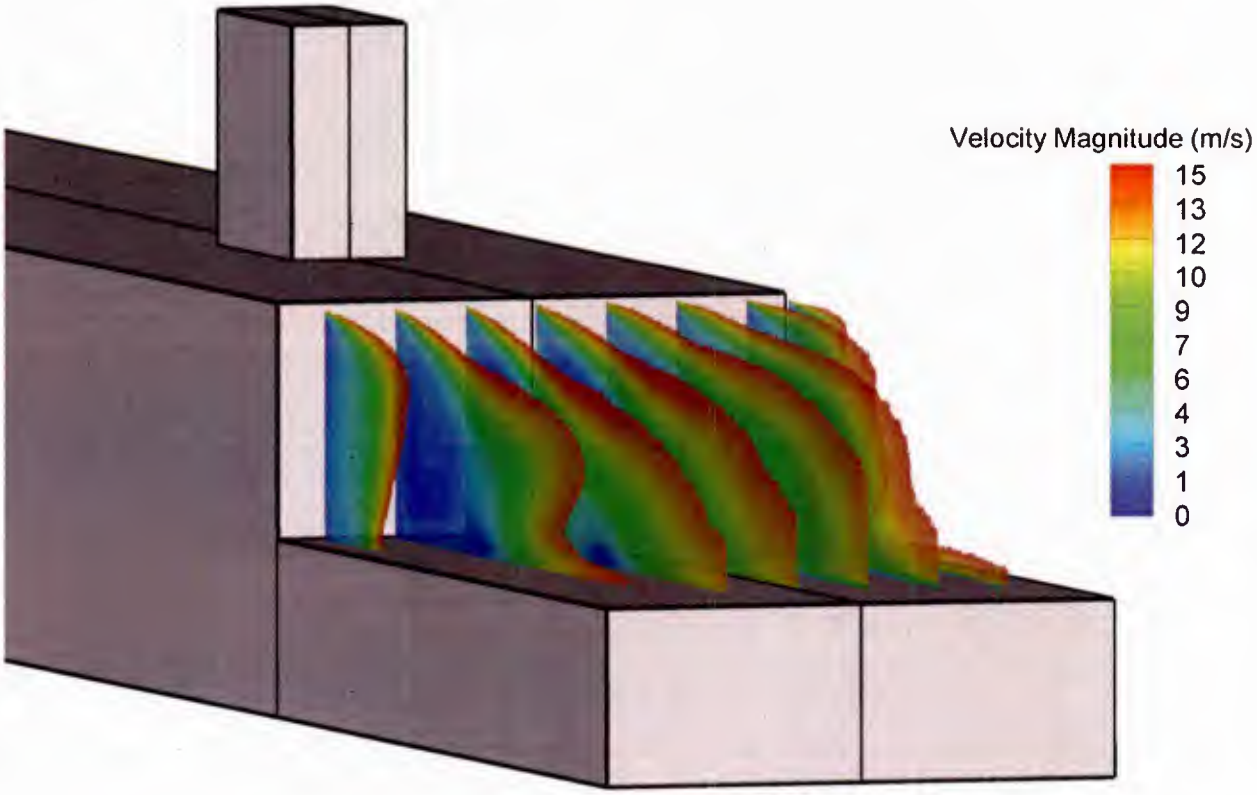

Figure 24. Time-averaged longitudinal plane PIV data (planes 2-9) over the flight deck.

SUMMARY AND OBSERVATIONS

A wind tunnel test to demonstrate PIV/SPIV capability to measure ship flowfield and airwake features in the NSWCCD SWT was successfully conducted. The implementation of PIV and SPIV in the SWT provided a detailed data set for the study of the flowfield and airwake of the SFS2 generic ship geometry. PIV and SPIV are available and ready for use in the SWT for tests requiring detailed flowfield measurements. The following summary and observations are noted:

1) High quality PIV and SPIV results can be obtained in the SWT using existing NSWCCD equipment with cameras mounted external to the SWT. Both longitudinal and lateral plane results were achieved. Existing PIV/SPIV expertise at NSWCCD was critical to the success of the test, and provides great confidence in conducting future successful PIV/SPIV test programs in the SWT for the Navy.

2) Excellent flow seeding in air is achieved with the TSI single-jet oil droplet generator, and its capacity is sufficient for our large wind tunnel.

3) A comparison of PIV longitudinal plane measurements over the flight deck to fast-response velocity probe data from a previous test of the same model and at the same

locations and test condition showed that there is good agreement between the velocity probes and the PIV measurements.

4) Flow features and flow structures pertaining to the ship flowfield and airwake were successfully measured and mapped using PIV and SPIV measurement techniques. Data were obtained for flow over the full length of the ship from bow to stern.

REFERENCES

1. Dai, Charles, Paisan Atsavapranee and David Fry, "Steady Turning Experiments for Model 5617 – Part(II) Stereo Particle Image Velocimetry Measurements", Hydromechanics Department Report, NSWCCD Carderock Division, May, 2011.

2. Rosenfeld, Nicholas C., Kevin R. Kimmel, and Anish J. Sydney, "Investigation of Ship Topside Modeling Practices for Wind Tunnel Experiments", AIAA-2015-0245, 53rd AIAA Aerospace Sciences Meeting, Kissimmee, FL Jan 5-9, 2015.

3. Quon, Eliot W., Philip A. Cross, Marilyn J. Smith, Nicholas C. Rosenfeld, and Glen R. Whitehouse, "Investigation of Ship Airwakes Using a Hybrid Computational Methodology", AHS 70th Annual Forum, Montreal, Quebec, May 20-22, 2014.

DISTRIBUTION

Organization	Hard Copies	Electronic Copies
DTIC	1	0

NSWCCD Internal Distribution

Code	Name	Hard Copies	Electronic Copies
6030	Jack Price	1	1
7301	Dan Goodwin	0	1
8010	Joe Gorski	1	1
8020	Monica Walker	1	1
8040	Art Reed	0	1
8070	Jessica Kleist	0	1
8100	Mike Wade	0	1
8200	Jeff Hough	0	1
8300	Brooks Darden	0	1
8400	Brian Heidt	0	1
8500	Jude Brown	1	1
8540	Rae Hurwitz	0	1
8540	Matt Marquardt	0	1
8600	David Armstrong	1	1
8600	Paisan Atsavapranee	1	1
8620	Emily Harrison	0	1
8630	Josh Rollins	0	1
8700	Acting	0	1
8800	Steve Ebner	1	1
8820	David Haas	1	1

NSWCCD Internal Distribution (continued)

Code	Name	Hard Copies	Electronic Copies
8820	Al Schwartz	0	1
8820	Kevin Kimmel	6	1
8820	Naipei Bi	0	1
8820	Joseph Ramsey	0	1
8820	Anish Sydney	0	1
3452	TIC	1	1
Total Number of Copies		**16**	**26**


UNITED STATES NAVY
SURFACE WARFARE CENTER